

## RESEARCH ARTICLE SUMMARY

## PLANETARY SCIENCE

# Pluto's interaction with its space environment: Solar wind, energetic particles, and dust

F. Bagenal,\* M. Horányi, D. J. McComas, R. L. McNutt Jr., H. A. Elliott, M. E. Hill, L. E. Brown, P. A. Delamere, P. Kollmann, S. M. Krimigis, M. Kusterer, C. M. Lisse, D. G. Mitchell, M. Piquette, A. R. Poppe, D. F. Strobel, J. R. Szalay, P. Valek, J. Vandegriff, S. Weidner, E. J. Zirnstein, S. A. Stern, K. Ennico, C. B. Olkin, H. A. Weaver, L. A. Young, New Horizons Science Team†

**INTRODUCTION:** The scientific objectives of NASA's New Horizons mission include quantifying the rate at which atmospheric gases are escaping Pluto and describing its interaction

## ON OUR WEB SITE

Read the full article at <http://dx.doi.org/10.1126/science.aad9045>

with the surrounding space environment. The two New Horizons instruments that measure charged particles are the Solar Wind Around Pluto (SWAP) instrument and the Pluto Energetic Particle Spectrometer Science Investigation (PEPSSI) instrument. The Venetia Burney Student Dust Counter (SDC) counts the micrometer-sized dust grains that hit the detectors mounted on the ram direction of the spacecraft. This paper describes preliminary results from these three instruments when New Horizons flew past Pluto in July 2015 at a distance of 32.9 astronomical units (AU) from the Sun.

**RATIONALE:** Initial studies of the solar wind interaction with Pluto's atmosphere suggested that the extent of the interaction depends on whether the atmospheric escape flux is strong (producing a comet-like interaction, where the interaction region is dominated by ion pick-up and is many times larger than the object) or weak (producing a Mars-like interaction dominated by ionospheric currents with limited upstream pick-up and where the scale size is comparable to the object). Before the New Horizons flyby, the estimates of the atmospheric escape rate ranged from as low as  $1.5 \times 10^{25}$  molecules  $\text{s}^{-1}$  to as high as  $2 \times 10^{28}$  molecules  $\text{s}^{-1}$ . Combining these wide-ranging predictions of atmospheric escape rates with Voyager and New

Horizons observations of extensive variability of the solar wind at 33 AU produced estimates of the scale of the interaction region that spanned all the way from 7 to 1000 Pluto radii ( $R_P$ ).

**RESULTS:** At the time of the flyby, SWAP measured the solar wind conditions near Pluto to be nearly constant and stronger than usual. The abnormally high solar wind density and associated pressures for this distance are likely due to a relatively strong traveling interplanetary shock that passed over the spacecraft 5 days earlier. Heavy ions picked up sunward from Pluto should mass-load and slow the solar wind. However, there is no evidence of such solar wind slowing in the SWAP data taken as near as  $\sim 20 R_P$  inbound, which suggests that very few atmo-

spheric molecules are escaping upstream and becoming ionized. The reorientation of the spacecraft to enable imaging of the Pluto system meant that both the SWAP and PEPSSI instruments were turned away from the solar direction, thus complicating our analysis of the particle data. Nevertheless, when the spacecraft was  $\sim 10 R_P$  from Pluto, SWAP data indicated that the solar wind had slowed by  $\sim 20\%$ . We use these measurements to estimate a distance of  $\sim 6 R_P$  for the 20% slowing location directly upstream of Pluto. At this time, PEPSSI detected an enhancement of ions with energies in the kiloelectron volt range. The SDC, which measures grains with radii  $> 1.4 \mu\text{m}$ , detected one candidate impact in  $\pm 5$  days around its closest approach, indicating a dust density estimate of  $n = 1.2 \text{ km}^{-3}$ , with a 90% confidence level range of  $0.6 < n < 4.6 \text{ km}^{-3}$ .

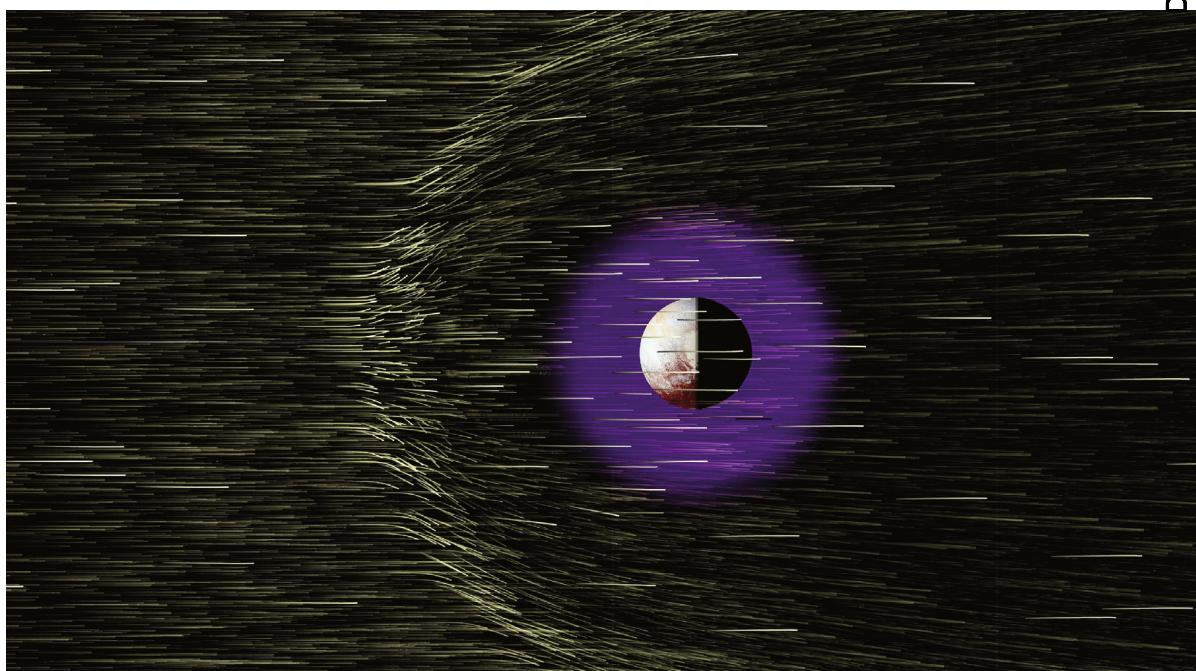
**CONCLUSION:** New Horizons's particle instruments revealed an interaction region confined sunward of Pluto to within  $\sim 6 R_P$ . The surprisingly small size is consistent with a reduced atmospheric escape rate of  $6 \times 10^{25}$   $\text{CH}_4$  molecules  $\text{s}^{-1}$ , as well as a particularly high solar wind flux due to a passing compression region. This region is similar in scale to the solar wind interaction with Mars's escaping atmosphere. Beyond Pluto, the disturbance persists to distances greater than  $400 R_P$  downstream. ■

The list of author affiliations is available in the full article online.

\*Corresponding author E-mail: [bagenal@colorado.edu](mailto:bagenal@colorado.edu)

†New Horizons Science Team authors and affiliations are listed in the supplementary materials.

Cite this article as F. Bagenal et al., *Science* **351**, aad9045 (2016). DOI: 10.1126/science.aad9045



**Interaction of the solar wind with Pluto's extended atmosphere.** Protons and electrons streaming from the Sun at  $\sim 400 \text{ km s}^{-1}$  are slowed and deflected around Pluto because of a combination of ionization of Pluto's atmosphere and electrical currents induced in Pluto's ionosphere.

## RESEARCH ARTICLE

## PLANETARY SCIENCE

# Pluto's interaction with its space environment: Solar wind, energetic particles, and dust

F. Bagenal,<sup>1,\*</sup> M. Horányi,<sup>1</sup> D. J. McComas,<sup>2,3</sup> R. L. McNutt Jr.,<sup>4</sup> H. A. Elliott,<sup>2</sup> M. E. Hill,<sup>4</sup> L. E. Brown,<sup>4</sup> P. A. Delamere,<sup>5</sup> P. Kollmann,<sup>4</sup> S. M. Krimigis,<sup>4,6</sup> M. Kusterer,<sup>4</sup> C. M. Lisse,<sup>4</sup> D. G. Mitchell,<sup>4</sup> M. Piquette,<sup>1</sup> A. R. Poppe,<sup>7</sup> D. F. Strobel,<sup>8</sup> J. R. Szalay,<sup>1,9</sup> P. Valek,<sup>2</sup> J. VandeGriff,<sup>4</sup> S. Weidner,<sup>2</sup> E. J. Zirnstein,<sup>2</sup> S. A. Stern,<sup>9</sup> K. Ennico,<sup>10</sup> C. B. Olkin,<sup>9</sup> H. A. Weaver,<sup>4</sup> L. A. Young,<sup>9</sup> New Horizons Science Team†

The New Horizons spacecraft carried three instruments that measured the space environment near Pluto as it flew by on 14 July 2015. The Solar Wind Around Pluto (SWAP) instrument revealed an interaction region confined sunward of Pluto to within about 6 Pluto radii. The region's surprisingly small size is consistent with a reduced atmospheric escape rate, as well as a particularly high solar wind flux. Observations from the Pluto Energetic Particle Spectrometer Science Investigation (PEPSSI) instrument suggest that ions are accelerated and/or deflected around Pluto. In the wake of the interaction region, PEPSSI observed suprathermal particle fluxes equal to about 1/10 of the flux in the interplanetary medium and increasing with distance downstream. The Venetia Burney Student Dust Counter, which measures grains with radii larger than 1.4 micrometers, detected one candidate impact in  $\pm 5$  days around New Horizons' closest approach, indicating an upper limit of  $<4.6$  kilometers<sup>-3</sup> for the dust density in the Pluto system.

**A**fter a journey of more than 9 years, NASA's New Horizons spacecraft flew past Pluto on 14 July 2015 (1). Scientific objectives of the New Horizons mission include quantifying the rate at which atmospheric gases are escaping Pluto (2) and describing its interac-

tion with the surrounding space environment. The two New Horizons instruments that measure charged particles are the Solar Wind Around Pluto (SWAP) instrument (3) and the Pluto Energetic Particle Spectrometer Science Investigation (PEPSSI) instrument (4). The Venetia Burney

Student Dust Counter (SDC) counts the micrometer-sized dust grains that hit the detectors mounted on the ram direction of the spacecraft (5). This paper describes preliminary results measured by these three instruments during the Pluto encounter period (the geometry of which is illustrated in Fig. 1). New Horizons reached its closest approach distance of  $11.54 R_P$ , where a Pluto radius is  $R_P = 1187$  km (1), on day of year (DOY) 195 at 11:49 universal time coordinated (UTC).

Initial studies of the solar wind interaction with Pluto's atmosphere (6–15), all assuming the absence of an intrinsic magnetic field, suggested that the extent of the interaction depends on whether the atmospheric escape flux is strong or weak: Strong escape flux produces a comet-like interaction, where the interaction region is dominated by ion pick-up and is many times larger than the object. Conversely, weak flux results in a Mars-like interaction dominated by ionospheric currents with limited upstream pick-up and where the scale size is comparable to that of the object. Before the New Horizons flyby, estimates of the atmospheric escape rate ranged from as low as  $1.5 \times 10^{25}$  molecules  $s^{-1}$  to as high as  $2 \times 10^{28}$  molecules  $s^{-1}$  (16–23). Combining these atmospheric escape rates with Voyager and New Horizons observations of the solar wind at 33 astronomical

<sup>1</sup>Laboratory of Atmospheric and Space Physics, University of Colorado, Boulder, CO 80600, USA. <sup>2</sup>Southwest Research Institute, San Antonio, TX 78228, USA. <sup>3</sup>University of Texas at San Antonio, San Antonio, TX 78249, USA. <sup>4</sup>Johns Hopkins University Applied Physics Laboratory, Laurel, MD 20723, USA. <sup>5</sup>University of Alaska, Fairbanks, AK 99775, USA. <sup>6</sup>Academy of Athens, 28 Panapistimiou, 10679 Athens, Greece. <sup>7</sup>Space Sciences Laboratory, University of California, Berkeley, CA 94720, USA. <sup>8</sup>Johns Hopkins University, Baltimore, MD 21218, USA. <sup>9</sup>Southwest Research Institute, Boulder, CO 80302, USA. <sup>10</sup>NASA Ames Research Center, Moffett Field, CA 94035, USA.

\*Corresponding author E-mail: bagenal@colorado.edu †New Horizons Science Team authors and affiliations are listed in the supplementary materials.

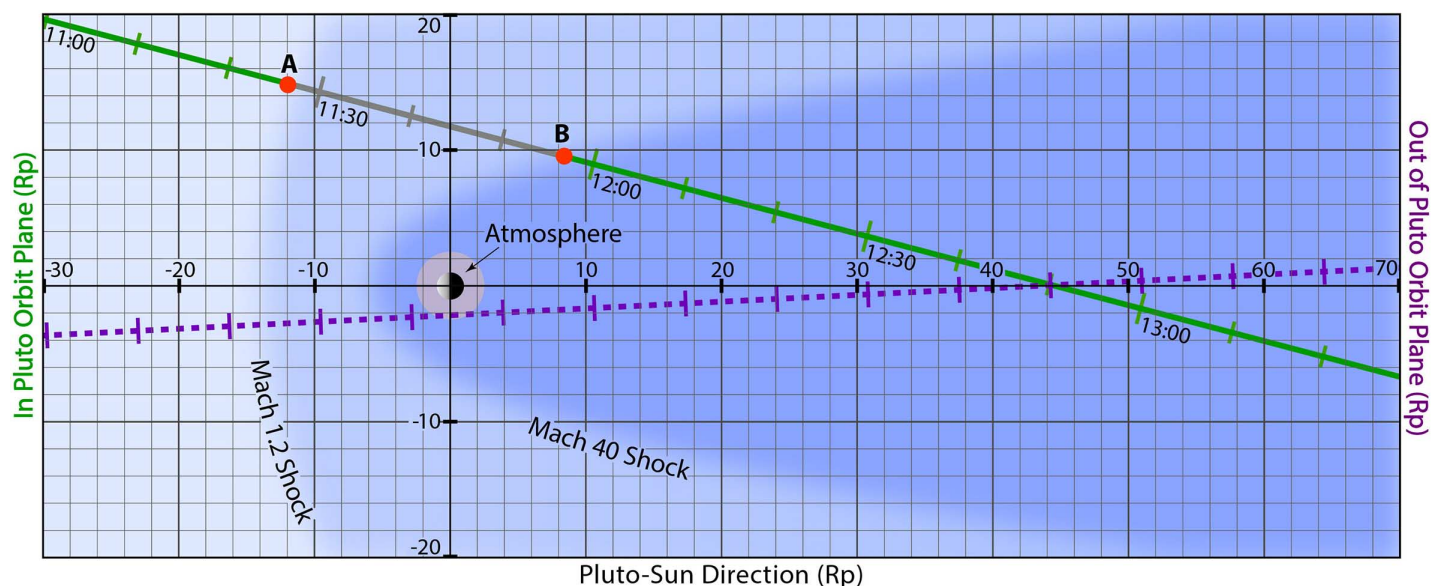


**Fig. 1. Geometry of the New Horizons trajectory through the solar wind interaction with Pluto's atmosphere on DOY 195.** Along the gray section of the trajectory between points A and B, the New Horizons spacecraft pointed the SWAP instrument's field of view away from the solar direction. The pink circle shows the extent of Pluto's atmosphere (2).



units (AU) produced estimates of the scale of the interaction region that ranged from 7 to 1000  $R_P$  (24).

New Horizons flew past Pluto at a distance of 32.9 AU from the Sun. At the time of encounter, Pluto was  $1.9^\circ$  above the ecliptic plane on its ec-

centric orbit. The flyby occurred as the Sun was in the descending phase of the solar cycle. In Table 1, we compare the interplanetary plasma

| Table 1. Solar wind conditions at 33 AU. Predictions are based on Voyager 2 plasma data obtained from 1988 to 1992 between 25 and 39 AU (24) and observed by the New Horizons SWAP instrument. $\gamma$ , adiabatic index; $m_i$ , ion mass. |   |                           |                       |                           |                  |
|--|---|---------------------------|-----------------------|---------------------------|------------------|
| Plasma property  | Formula [units]                         | Predicted 10th percentile | Predicted mean        | Predicted 90th percentile | Observed by SWAP |
| Solar wind speed   | $V_{SW}$ [km/s]                         | 380                       | 430                   | 480                       | 403              |
| Proton density   | $n$ [cm $^{-3}$ ]                       | 0.0020                    | 0.0058                | 0.014                     | 0.025            |
| Proton flux  | $nV$ [km s $^{-1}$ cm $^{-3}$ ]         | 0.84                      | 2.4                   | 7.0                       | 10               |
| Proton temperature   | $T$ [K]<br>$T$ [eV]                     | 3040<br>0.26              | 6650<br>0.57          | 16800<br>1.5              | 7700<br>0.66     |
| Proton thermal pressure (IPUI pressure*)   | $P = nkT$ [fPa]                         | 0.12                      | 0.53<br>(20 $\pm$ 8*) | 2.1                       | 2.5              |
| Proton ram pressure  | $P = \rho V^2$ [pPa]                    | 0.55                      | 1.7                   | 4.0                       | 6.0              |
| Sound speed (with IPUIs*)  | $V_s = (\gamma kT/m_i)^{1/2}$ [km/s]    | 6.3                       | 9.4<br>(58*)          | 15                        | 10<br>(28*)      |
| Sonic Mach number (with IPUIs)   | $M_s = V_{SW}/V_s$                      | 60                        | 46<br>(7.5*)          | 32                        | 40<br>(14*)      |
| Magnetic field strength  | $B$ [nT]                                | 0.08                      | 0.15                  | 0.28                      | 0.3†             |
| Pickup CH $_4^+$ gyroradius  | $R_{gyro}$ [ $R_P$ ]                    | 670                       | 400                   | 240                       | 190†             |
| Alfvén speed   | $V_A = B/(\mu_0 \rho)^{1/2}$ [km/s]     | 22                        | 45                    | 96                        | 41†              |
| Alfvén Mach number   | $M_A = V_{SW}/V_A$                      | 4.6                       | 9.5                   | 20                        | 9.8†             |
| Magnetosonic Mach no. (with IPUIs*)  | $M_{MS} = V_{SW}/(V_A^2 + V_s^2)^{1/2}$ | 17                        | 9<br>(6*)             | 5                         | 9.5†<br>(8*†)    |

\*Including the thermal pressure of IPUIs from (31, 32, 56). †For the Pluto flyby, we take an interplanetary magnetic field strength of  $\sim 0.3$  nT.

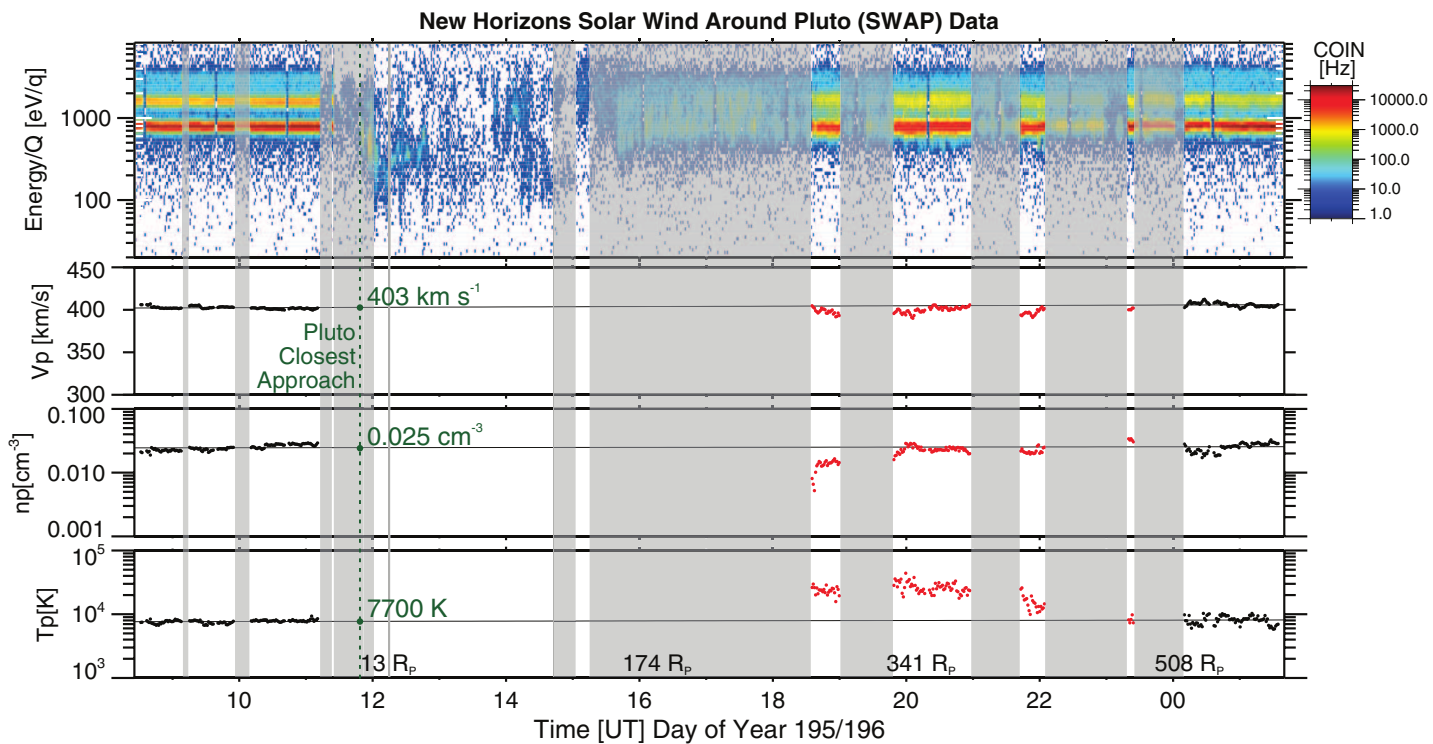


**Fig. 2. Overview of SWAP data.** Color spectrogram of coincidence count rate (COIN) as a function of  $E/q$  and derived proton flow speed, density, and temperature values for the interval surrounding the Pluto flyby. The vertical dashed green line shows the time of closest approach. Unshaded regions indicate times during which some portion of SWAP's very broad field of view was pointed within  $5^\circ$  of the Sun direction, and thus SWAP would be able to observe a radially outflowing solar wind. Moments are derived for these times when solar wind-like distributions were observed. Black data points at the start and end of this interval allow linear least-squares fits to these samples of essentially pristine solar wind (nearly horizontal lines), whereas disturbed, higher-temperature solar wind (red points) is evident in the interaction region several hundred  $R_P$  behind Pluto.

conditions predicted based on Voyager data for 33 AU (24) with the observations made by the New Horizons SWAP instrument. In the absence of a direct measurement of the local magnetic field, we assume an interplanetary magnetic field (IMF) of 0.3 nT, at the upper end of the range observed by Voyager (as discussed further below).

### Solar Wind Around Pluto The SWAP instrument

The SWAP instrument was specifically designed and optimized for the New Horizons mission, with the primary design drivers being (i) a large aperture and geometric factor to accurately measure the tenuous solar wind at ~33 AU, (ii) minimum use of spacecraft resources such as mass and power, and (iii) its position mounted on a spacecraft that would rotate over a very wide range of spacecraft-pointing directions throughout the flyby. Early in the mission development phase, the flyby-pointing directions were not well known, but the best information available at that time was that most spacecraft pointing would involve rotation around a single spacecraft axis: the  $z$  axis. Thus, SWAP was designed to have an extremely broad acceptance angle (~276°) in the plane perpendicular to this axis, which requires an electrostatic top-hat style analyzer with its axis of symmetry aligned with the spacecraft's  $z$  axis. Ions are bent through the electrostatic analyzer, pass through a nearly field-free conical region, and are focused into a coincidence detector section, which provides very high signal-to-noise ratio measurements for solar wind ions. Details of the SWAP instrument design are provided by McComas *et al.* (3), and SWAP data has already been used to examine the Jovian magnetosphere and distant magnetotail (25–29).

### The solar wind at the time of the Pluto flyby

At the time of the flyby, the solar wind conditions near Pluto (measured by SWAP) were nearly constant, which is advantageous for interpreting the solar wind–Pluto interaction. The top panel of Fig. 2 shows a color spectrogram of SWAP coincidence counts as a function of energy per charge ( $E/q$ ) and time. On the left and right sides of the plot, away from the Pluto interaction, the red and yellow bands located slightly under 1 and 2 keV/ $q$  are solar wind protons and alpha particles, respectively. We calculate the solar wind proton parameters for these intervals (30) and find a strong consistency between the values before ~11:20 UTC on DOY 195 and again on DOY 196 (black points). These intervals represent the unperturbed solar wind ahead of and beyond Pluto along the New Horizons trajectory, respectively. Interpolating between these points (black line), we infer—at the time of the New Horizons's closest approach (11:48 UTC; green vertical dashed line)—a solar wind speed of ~403 km s<sup>-1</sup>, a proton density of ~0.025 cm<sup>-3</sup>, a proton temperature of ~7700 K (0.7 eV), a proton dynamic pressure of ~6.0 pPa, and a core solar wind proton thermal pressure of ~2.5 × 10<sup>-3</sup> pPa (Table 1). From the properties of just the thermal solar wind, we calculate a sonic

Mach number of ~40. The sonic Mach number is substantially reduced to 14 if we include the interstellar pick-up ions (IPUIs), which provide thermal pressure that is roughly an order of magnitude greater than the aforementioned value at these heliocentric distances (31, 32). The measured unusually high solar wind density and associated pressures for this distance are probably due to a relatively strong traveling interplanetary shock that passed over the spacecraft 5 days earlier on DOY 190.

New Horizons was not equipped with a magnetometer, so the interplanetary magnetic field strength at the time of the flyby is not known. In Table 1, we list typical values of the IMF magnitude ( $|B|$ ) of 0.08 to 0.3 nT at 33 AU in the solar wind (24, 33). If we assume the interplanetary shock that passed New Horizons on DOY 190 also

increased  $|B|$  to the top of this range, we calculate an Alfvén speed [ $V_A = B/(\mu_0 \rho)^{1/2}$ , where  $\mu_0$  is the vacuum permeability and  $\rho$  is the total mass density of the charged plasma particles] of 41 km s<sup>-1</sup>; an Alfvén Mach number ( $M_A = V_{SW}/V_A$ ; where  $V_{SW}$  is the solar wind speed) of 9.8; and a magnetosonic Mach number [ $M_{MS} = V_{SW}/(V_A^2 + V_s^2)^{1/2}$ , where  $V_s$  is the speed of sound] of 9.5, which is reduced to 8 if we include the IPUIs. The ratio of proton thermal pressure to magnetic pressure [ $\beta = nkT/(B^2/2\mu_0)$ ; where  $n$  is the proton density,  $k$  is Boltzmann's constant, and  $T$  is temperature] is just 0.07, which appears to suggest that the IMF dominates the dynamics. But if we include the substantial pressure of the IPUIs,  $\beta$  becomes greater than unity, emphasizing the importance of IPUIs for the dynamics of the outer heliosphere. We stress that all of these values are based

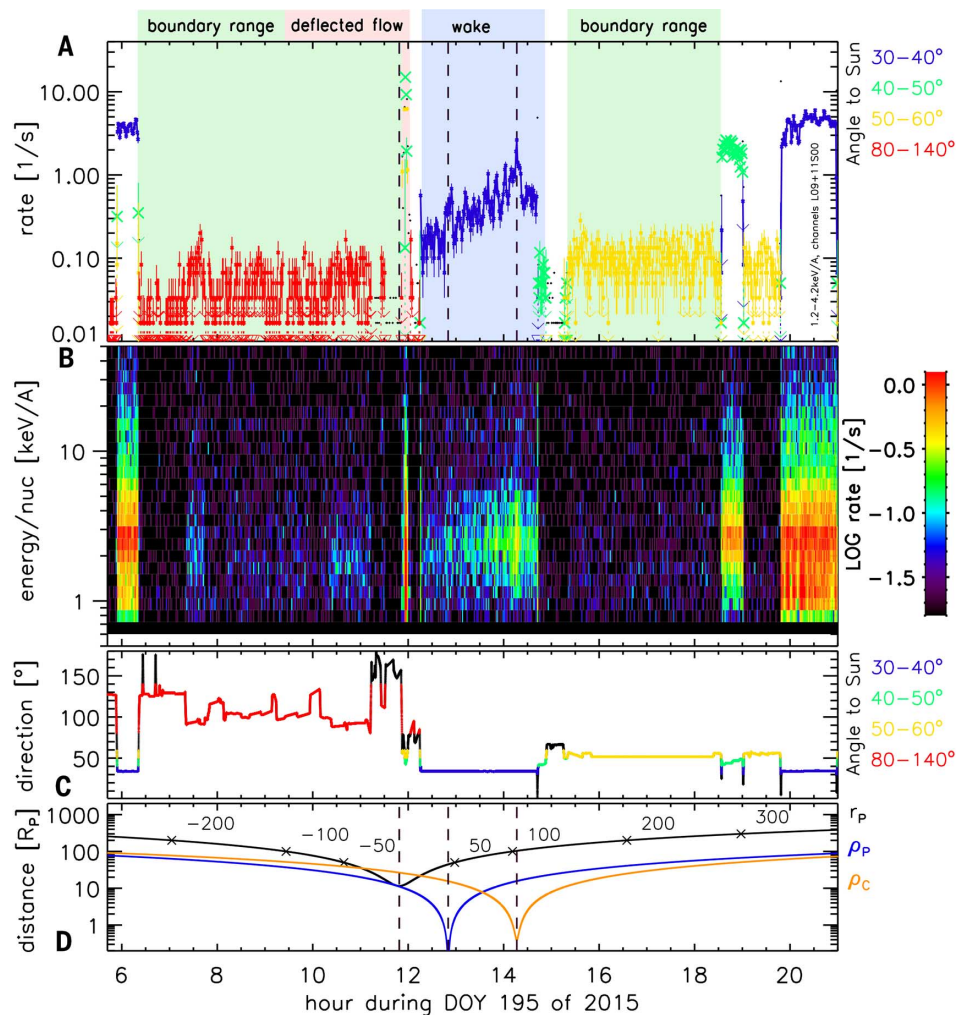


**Fig. 3. Overview of PEPSSI data taken near Pluto.** (A) Measurement of ions with Poisson error bars based on TOF data. Ion speeds inside the instrument correspond to 1 to 4 keV/amu. The colors of the symbols identify the viewing angles relative to the Sun direction (D). Background colors refer to time periods discussed in the text. Dashed lines denote locations where New Horizons had its closest approach to Pluto and was directly antisunward of Pluto and Charon. (B) Energy spectrogram of TOF data, assuming that ions have not been accelerated by the potential but not accounting for energy losses in the foils. (C) Angle of PEPSSI's sector S0 to the Sun direction, with colors corresponding to those used in (A). (D) Location of New Horizons relative to Pluto and Charon. Black, radial distance to Pluto; blue, distance along the Pluto–Sun line; red, distance to the Pluto–Sun line; orange, distance to the Charon–Sun line.

on assumed field strengths and not measured values.

### Upstream interaction confined close to Pluto

Heavy ions picked up sunward from Pluto should mass-load and slow the solar wind ahead of it. However, there is no evidence of such solar wind slowing and hence no evidence of the addition of Pluto pick-up ions (PPUIs) in the SWAP data as

close as  $\sim 20 R_P$  inbound (point A in Fig. 1 at 11:25 UTC). The calculated speed value at that location is  $405 \text{ km s}^{-1}$ , but if we take an upper bound of 1% slowing at this point, or  $399 \text{ km s}^{-1}$  compared with the interpolated value at Pluto of  $403 \text{ km s}^{-1}$ , we can use conservation of momentum to calculate an upper bound on the density of a fully picked up heavy ion [ $\text{CH}_4$  (2)] at this distance. We note that if the pick-up ions are  $\text{N}_2$  instead of  $\text{CH}_4$ , densities would be smaller by the mass ratio

of the ions [28 atomic mass units (amu)/16 amu = 1.75]. For a solar wind proton density of  $0.025 \text{ cm}^{-3}$ , we obtain

$$403 \text{ km s}^{-1} \times 0.025 \text{ cm}^{-3} = 399 \text{ km s}^{-1} \times 0.025 \text{ cm}^{-3} (1 + 16N_{\text{CH}_4}/N_p)$$

providing an upper bound on the  $N_{\text{CH}_4}/N_p$  ratio (number of  $\text{CH}_4$  molecules/number of protons) of  $\sim 6 \times 10^{-4}$  and upper bound on the fully picked up  $\text{CH}_4$  density of  $2 \times 10^{-5} \text{ cm}^{-3}$  at  $20 R_P$  along the New Horizons trajectory.

Between 11:25 and 11:56 UTC, the New Horizons spacecraft was pointed in directions that did not allow SWAP to view back toward the Sun and into the solar wind. However, from 11:56 to 11:58 UTC (point B in Fig. 1), the spacecraft rotated through directions sufficiently close to the sunward direction such that SWAP was able to take three contiguous energy-per-charge scans of what appears to be solar wind plasma. For each sample, we made Gaussian fits around the peak of the coincidence counts, including errors, and calculated speeds of 314, 343, and  $315 \text{ km s}^{-1}$ , for an average of  $324 \text{ km s}^{-1}$ . Therefore, we conclude that the solar wind had slowed by  $\sim 20\%$  at this location. Repeating the conservation of momentum calculation as above

$$403 \text{ km s}^{-1} \times 0.025 \text{ cm}^{-3} = 324 \text{ km s}^{-1} \times 0.025 \text{ cm}^{-3} (1 + 16N_{\text{CH}_4}/N_p)$$

produces an approximate  $N_{\text{CH}_4}/N_p$  ratio of  $\sim 2 \times 10^{-2}$  and a fully picked up  $\text{CH}_4$  density of  $\sim 4 \times 10^{-4} \text{ cm}^{-3}$  at this location along Pluto's dawn flank. This very small amount of mass loading so close to Pluto demonstrates that Pluto cannot have a strong comet-like interaction as was generally thought before the flyby.

### Extended interaction behind Pluto

For roughly 3 hours after its closest approach to Pluto, SWAP observed much lower levels of coincidence counts and no obvious beamlike distribution characteristic of the solar wind. From

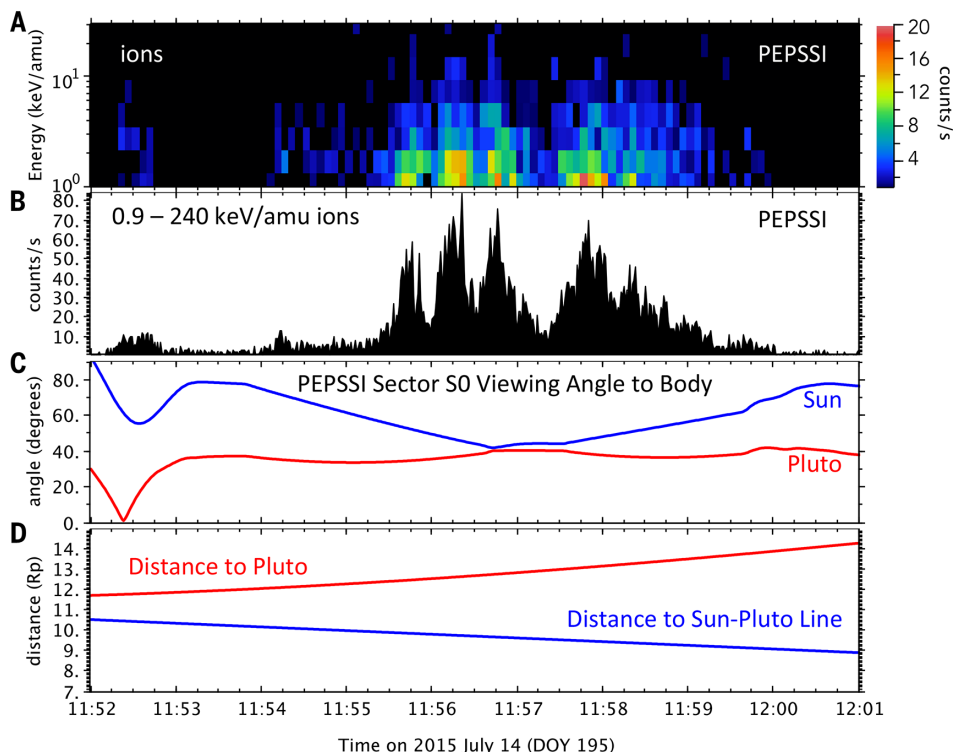


**Fig. 4. Burst of energetic ions.** Zooming in to the interval shaded pink in Fig. 3A, we show PEPSSI TOF observations from 11:52 to 12:01 UTC on 14 July 2015. (A) Color spectrogram of 6625 single TOF events returned during this period from all PEPSSI sectors. Raw data are acquired once every second and have been binned into 5-s average rates and logarithmically spaced bins in energy per mass. (B) Corresponding total counts per second integrated across all energies. (C) Angle between the direction to the Sun and the normal to the S0 sector. (D) Distance of New Horizons to Pluto and to the Sun-Pluto line during this period.

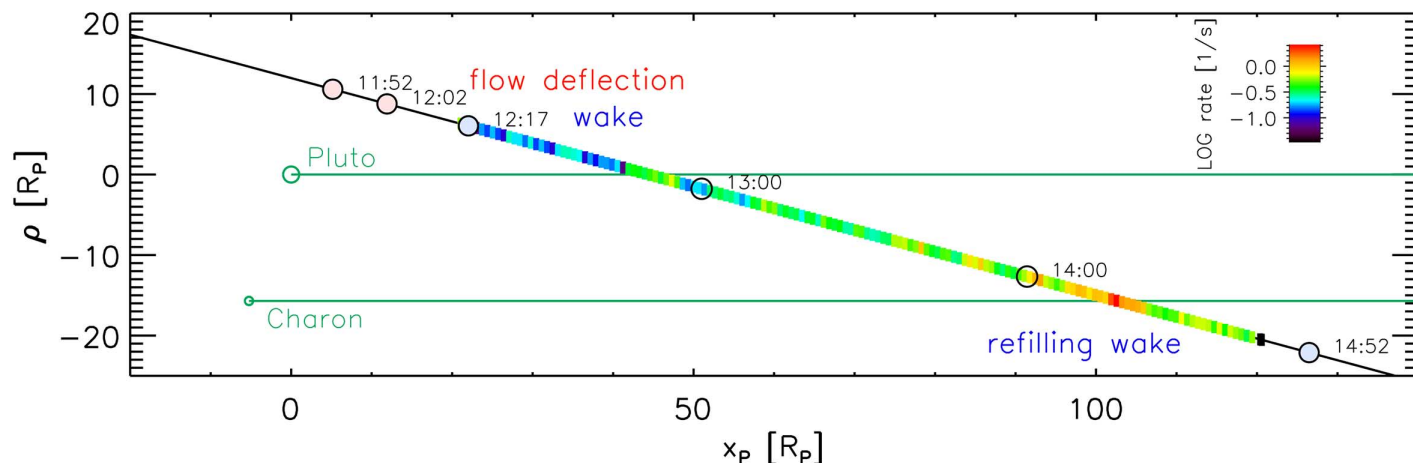


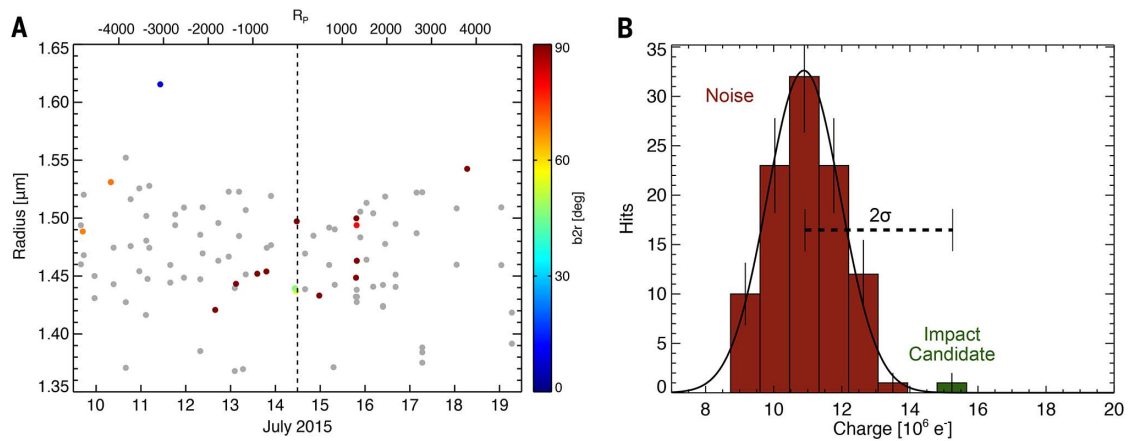
**Fig. 5. Energetic particles along the trajectory of New Horizons.** The  $x_P$  axis points away from the Sun. The vertical axis shows  $\rho_P$ , the distance from the  $x_P$  axis in a plane containing Pluto and the trajectory. Green circles show the locations of Pluto and Charon. Open circles show times in UTC. Pink-filled circles mark the range of the ion enhancement; blue-filled circles delimit the wake. Color along the trajectory shows a PEPSSI count rate (same as in Fig. 3A).



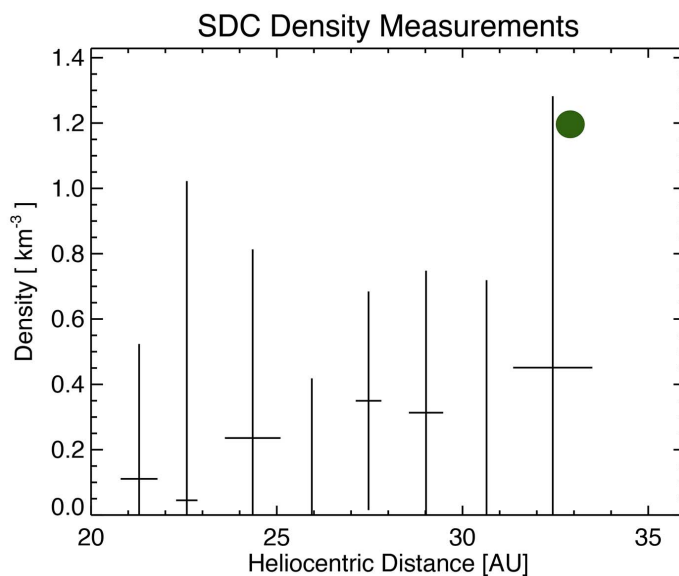
**Fig. 6. Events around Pluto.**

(A) The events recorded during  $\pm 5$  days of the closest approach to Pluto. Gray colored dots indicate noise events identified to be coincident dust hits or a single event coincident with thruster firings. The color code represents the boresight-to-ram angle ( $b_2r$ ), measured between the SDC surface normal and the velocity vector of the spacecraft. SDC's sensitivity rapidly drops to zero for impact angles  $>45^\circ$ ; hence,

events marked by red and green dots are also noise events. A single detection at a distance of  $\sim 3000 R_P$  (11 July 2015), before the closest encounter remains, the only candidate for detecting a Pluto-system dust particle. (B) The amplitude distribution of all the noise events during this period is well fit to a Gaussian curve with an average of  $1.1 \times 10^7 e$  and a  $1\sigma$  error =  $1.5 \times 10^6 e$ , indicating that our candidate impact event generated a charge that had an amplitude with a  $2\sigma$  error above the average.

**Fig. 7. Dust in the outer solar system.**

The image shows dust density or particles with radii  $>1.4 \mu m$ , as measured by SDC in the outer solar system. The last data point with an error bar shows the data collected since 1 January 2015. The green dot indicates the most likely dust density of  $1.2 km^{-3}$ , on the basis of a single candidate dust event.



$\sim 12:00$  to  $14:40$  UTC and again from  $\sim 15:00$  to  $15:15$  UTC (unshaded regions in Fig. 2), SWAP was viewing close enough to the sunward direction to see such a beam. However, because (i) a relatively narrow, solar wind-like distribution could have been deflected in this region, and (ii) sufficiently slow-flowing solar wind plasma would drop below the energy range sampled by SWAP, it is not possible to determine from these coincidence data whether the solar wind was somehow excluded from all or part of the sampled region and/or whether it was simply flowing in a way that SWAP was not able to observe. More detailed analysis of the SWAP data, including identification of the light (solar wind) versus heavy (Pluto) ions will be required to understand the plasma distributions observed behind Pluto.

Starting at  $\sim 18:30$  UTC, New Horizons was turned several times to observe the solar wind direction, and SWAP measured disturbed solar wind with somewhat variable speed and density

and proton temperatures up to  $\sim 40,000$  K ( $3.4 eV$ ), much higher than the  $\sim 7700$  K ( $0.7 eV$ ) of the surrounding solar wind. As seen in Fig. 2 (red points), the temperature shows elevated values that generally drop off with distances greater than  $400 R_P$  and return to the essentially unperturbed values by around the start of DOY 196. These SWAP observations suggest substantial heating by the Pluto interaction. Finally, by the time that New Horizons next viewed the solar wind at the start of DOY 196, the plasma conditions had essentially returned to those observed before the flyby, indicating the end of any noteworthy interaction with Pluto.

### Particle measurements The PEPSSI instrument

The PEPSSI instrument measures the time of flight (TOF) of energetic ions and electrons by detecting their passage between start and stop foils. For particles with sufficiently high energy,

the energy deposited in a given solid-state detector is measured (4). PEPSSI has six angular sectors labeled S0 to S5, and we concentrate on the measurements in S0, which observes particles close to the Sun direction during the time of the Pluto encounter. We report on TOF-only ion measurements corresponding to an energy per mass of  $\sim 0.5$  to  $50 keV/amu$ , for which PEPSSI observed the highest counting rates at Pluto. The PEPSSI TOF range nominally extends from 3 to 168 ns (34) for time intervals reported for ions traversing a 6.00-cm path internal to the instrument.

Ions are accelerated into PEPSSI by a potential of  $\sim 2.63$  kV by a negatively biased grid at the entrance apertures. This potential is with respect to the spacecraft, which we assume to be close to that of the ambient plasma. The reported energy/mass range given above is measured inside the instrument. Without knowledge of an ion's mass, there is ambiguity about what ion species are being measured. The likely composition of ions in the solar wind in the outer heliosphere includes  $H^+$ ,  $He^{++}$ ,  $He^+$ , and  $O^{7+}$ , either from the ions originating in the solar corona (35) or from IPIs originating in the interstellar medium (36).

### PEPSSI observations of the Pluto environment

Pluto has a substantial effect on the interstellar pickup and suprathermal ions, as illustrated in Fig. 3. We have found no decisive evidence for plutogenic heavy ions in the PEPSSI energy range in the immediate vicinity of Pluto (within  $500 R_P$  of Pluto). There were also no detections near Pluto of  $>25$ -keV electrons above a background consistent with the expected galactic cosmic ray fluxes.

Figure 3 shows an overview of the PEPSSI measurements obtained during the Pluto flyby. New Horizons entered the region of Pluto's interaction, as seen in the energetic particles sometime between 06:20 and 11:52 UTC on the flyby day. PEPSSI data suggest that New Horizons left the

Pluto interaction region sometime between 15:20 and 18:33 UTC, equivalent to a downstream distance of 120 to 270  $R_P$ . These periods are marked by green background shading in Fig. 3. The energetic particles return to a normal state after 18:33 UTC. The earliest and latest times delimit periods using two criteria: when PEPSSI was close to its nominal attitude (sector S0 of the instrument pointed  $\sim 35^\circ$  from the Sun direction) and when measured fluxes and spectra were characteristic of those observed in the interplanetary medium.

Around 11:57 UTC (point B in Fig. 1) and  $50^\circ$  from the solar direction, PEPSSI detected intensities  $>10$  times larger than those typically observed for that attitude. At that time, New Horizons was  $\sim 10 R_P$  to the side of Pluto. Figure 4 shows a close-up of this time period. The envelope of the measured intensities is modulated by the change in PEPSSI's look direction, and there is a superimposed fine structure on the time scale of several seconds (corresponding to  $\sim 0.1 R_P$ ). This fine structure, together with the higher-than-normal intensities for this look direction, suggests that New Horizons entered a new region. One hypothesis is that PEPSSI detects particles accelerated from lower energies at a compressive shock near Pluto. Such a shock might be similar to the exotic shock observed at Titan in the solar wind (37). Moreover, the TOF spectrum at that time is too similar to measurements in the interplanetary medium (compare to Fig. 3) to make this scenario likely. Another hypothesis is that the intensity enhancements result from the flow being deflected closer to the PEPSSI field of view, and that the fine structure reflects rapid changes associated with the flow being turbulent about this mean deflection. This interpretation has the virtue of simultaneously explaining the similarity of the spectra and difference in the direction relative to the Sun, as well as the position of the enhancement relative to Pluto.

From at least 12:15 to 14:42 UTC (to at least  $100 R_P$  downstream; compare with Fig. 3), New Horizons was in a region very different from that observed in the interplanetary medium, which we assume to be a wake downstream of Pluto. Although PEPSSI was in its nominal attitude favorable for measuring pick-up ions, the intensities at TOFs equivalent to  $\sim 1$  to 4 keV/amu were  $\sim 10$  times lower than in the surrounding interplanetary medium. We note that the intensity but not the spectral shape appear to be changing over time. The color scale along the trajectory curve in Fig. 5 shows a gradual increase in count rate during this period as the spacecraft departs from Pluto. It is the distance from Pluto, not the distance away from the Sun-Pluto line, that organizes the intensification trend. The TOF observations show a break in the energy spectrum, at an energy similar to comparable instances in the interplanetary medium.

The ion intensity throughout the wake exhibits its 20-min quasi-periodic enhancements superposed on the overall trend. These might be a result of turbulent flow within the wake, similar to the possible deflected flow interpretation of

observations closer to Pluto, but the scale is much larger in the wake. Two of these enhancements are broader, with sharp peaks in their center, and coincide with New Horizons passing the geometric wakes of Pluto and Charon. Figures 3 and 5 show these enhancements at 12:50 UTC, when New Horizons was  $44 R_P$  downstream of Pluto, and at 14:17 UTC, when it was  $97 R_P$  downstream of Charon. These enhancements are reminiscent of measurements at 12 to 25 lunar radii downstream of Earth's Moon, immersed in the solar wind and magnetosheath (38). At the Moon, there is a density enhancement on the central axis of the wake where protons refilling the wake parallel and antiparallel to the magnetic field merge together.

PEPSSI data reveal an interaction between Pluto and the solar wind, with a scale of at least  $11 R_P$  on the flank of Pluto and extending at least  $84 R_P$  downstream in the solar wind when the spacecraft attitude changed to an unfavorable orientation for PEPSSI observations before completely exiting the Pluto interaction region.

### Dust measurements at Pluto The SDC

The SDC is an impact dust detector onboard the New Horizons spacecraft. SDC measures the mass of dust grains in the range of  $10^{-12} < m < 10^{-9}$  g, covering an approximate size range of 0.5 to 10  $\mu\text{m}$  in particle radius (5). Since April 2006, SDC has been taking near-continuous measurements across the solar system (39, 40) and has already provided estimates for the dust production rate and initial size distribution of dust in the Edgeworth-Kuiper belt (41, 42). SDC is the first dedicated dust instrument to reach beyond 18 AU.

To optimize its observations during the Pluto encounter, New Horizons executed a complicated sequence of attitude changes by firing its thrusters. To avoid recording excessive noise during the encounter, on 1 January 2015 we set our charge threshold to  $Q \sim 10^7 e$  (where  $e$  is the electron charge), corresponding to a smallest detectable particle radius of 1.4  $\mu\text{m}$ . This charge threshold is above the level of the majority of SDC-recorded thruster events throughout the mission. The thresholds were reset to their pre-encounter values on DOY 211 in 2015.

### Dust measurements during the encounter

A period of  $\pm 5$  days centered on New Horizons's closest approach, corresponding to approximately  $\pm 5000 R_P$ , is used to calculate the dust density distribution of the Pluto system. SDC recorded a total of 102 events in this time period. Throughout the mission, due to the expected low dust fluxes, coincident events between multiple channels or events coincident with thruster firings were identified as noise events for both the exposed and the reference detectors. Figure 6 shows all of the recorded events throughout the encounter.

After identifying the coincident events as noise, 16 events remained as candidate dust hits. None

of these events occurred on the two reference detectors. New Horizons passed through the Pluto system with a speed of  $v_{s/c} \sim 14$  km/s relative to Pluto. Dust grains in the Pluto system are expected to have speeds  $< v_{s/c}$ ; hence, to a good approximation,  $v_{s/c}$  becomes the impact speed. Due to the sequence of observations executed by New Horizons, the orientation of the spacecraft changed almost continuously during the encounter, pointing SDC only intermittently in the ram direction. Because of the impact angle dependence of SDC's sensitivity, the detection probability of dust particles with impact angles  $> 45^\circ$  approaches 0, and these events are also identified as noise. Throughout the entire period of the close encounter, SDC recorded only a single large amplitude event that could be attributable to a dust impact. To assess to probability that this event was not noise, we examined the amplitude distribution of the recorded noise events and estimated that the detection is outside the  $2\sigma$  error of the average amplitude of the noise events. Hence, the probability that this event is a dust particle is  $\sim 95\%$ . We use this single detection as an upper limit to estimate the dust density near Pluto (see supplementary materials), indicating that the density is most likely  $1.2 \text{ km}^{-3}$  and the 90% confidence level for the density is in the range of  $0.6 < n < 4.6 \text{ km}^{-3}$ .

Figure 7 compares this density estimate with dust measurements in the outer solar system, indicating that the dust density of particles with radii  $> 1.4 \mu\text{m}$  remained within a  $1\sigma$  error of our last data point representing the SDC measurements since 1 January 2015.

The plasma wave instruments on Voyager 1 and 2 also showed a roughly flat dust density of  $\sim 0.2 \text{ km}^{-3}$ , though in that case the size of the detected particles remained poorly determined (43). This match can now be used to estimate that the Voyager dust detection threshold is similar to that of SDC during the Pluto flyby.

The dust density distribution perhaps indicates a slight increase with distance. This could be the result of the inner edge of the Kuiper belt dust disk extending inward and engulfing the outer solar system. Alternatively, the dust density increase could be local to the Pluto system. As SDC will map the dust density distribution for years to come, we will learn how the trend continues deep into the Kuiper belt.

### Discussion

#### The obstacle Pluto presents to the solar wind

Pluto presents an unusual obstacle to the solar wind, and any theory that seeks to explain it has to account simultaneously for a challenging range of observations provided by New Horizons. In particular, the SWAP observations of limited ( $< 1\%$ ) slowing of the solar wind at  $\sim 20 R_P$  upstream of Pluto (point A in Fig. 1) suggest that very few atmospheric molecules are escaping, becoming ionized, and mass-loading the solar wind. When the spacecraft was  $8.8 R_P$  tailward and at a transverse distance of  $9.6 R_P$  from Pluto (point B in Fig. 1), the solar wind

had slowed by ~20%. At this time, PEPSSI detected an enhancement of ions with energies in the kilo-electron volt range. Although there is no current consensus on the nature of the interaction boundary, we can still estimate its size. We can make a zero-order calculation of the size of the Pluto obstacle to the solar wind by assuming the same transverse distance applies at Pluto's terminator and multiplying by two-thirds (on the basis of experience at terrestrial planets) to get a very approximate distance of  $\sim 6 R_P$  for the 20% slowing location directly upstream of Pluto. This distance is about twice as large (scaled to the planet) as the maximum observed bow shock distance in the terminator plane for Mars and Venus (44). The interaction at Pluto is therefore consistent with a Mars-like interaction, given the current uncertainties in its bow shock location.

The solar wind interaction with Pluto's atmosphere is expected to depend on (i) the solar wind flux at Pluto, which varies by a factor of 10 on time scales of a few days and by  $1/a^2$  with Pluto's heliocentric distance  $a$ ; (ii) the escape rate of Pluto's neutral atmosphere; and (iii) the ionization rate of Pluto's atmosphere, which, for both photoionization and charge-exchange, also varies by  $1/a^2$ . The enhanced solar wind pressure (due to recent passage of an interplanetary compression region) at the time of the Pluto encounter suggests that the interaction region was in a compressed state at the time of the New Horizons flyby.

If the obstacle is mass-loading the solar wind via ionization of an escaping atmosphere, then we would expect the size of the obstacle to be inversely proportional to the upstream solar wind momentum flux. Comparing the observed solar wind flux with typical Voyager 2 values (Table 1), the factor of  $\sim 4$  enhancement at the time of the New Horizons flyby suggests that more typical size range for the obstacle (for the same atmospheric escape rate) would be  $\sim 25 R_P$ .

On the other hand, if the solar wind does not suffer substantial mass loading due to ionization of an escaping neutral atmosphere well upstream of the object, the solar wind will be slowed by ion pick-up (and subsequent mass-loading) in the outer atmosphere and diverted by electrical currents induced in Pluto's ionosphere. The size of such an interaction, similar in nature to Mars and Venus, is set by the altitude of the peak ionospheric electron density and how sharply the atmospheric density drops with altitude. This Mars-type interaction of the solar wind with an exosphere or ionosphere would be less compressible and would fluctuate less in size with solar wind flux.

Whereas the small size of the interaction region relative to the Pluto is reminiscent of Mars and Venus, recent observations of the solar wind interaction with the relatively weakly outgassing comet 67P Churyumov-Gerasimenko by instruments on ESA's Rosetta spacecraft (45–47) show deflection of the solar wind with a relatively modest decrease in speed. We anticipate productive discussions of the relative roles of atmospheric escape rate, solar wind flux, and IMF strength at

Mars, comet 67P, and Pluto as the data from the MAVEN (Mars Atmosphere and Volatile Evolution), Rosetta, and New Horizons spacecraft are further analyzed.

### Atmospheric escape

Pluto's atmosphere was first detected in 1988 during stellar occultation (48) and was later determined to be primarily composed of  $N_2$  with minor abundances of  $CH_4$  and  $CO$ , with surface pressures of  $\sim 17 \mu\text{bar}$  (49, 50). Pluto's low gravity implies that a large flux of atmospheric neutrals can escape. Estimates of escape rates range from as low as  $1.5 \times 10^{25}$  molecules  $s^{-1}$  to as high as  $2 \times 10^{28}$  molecules  $s^{-1}$ . The most recent (pre-New Horizons) atmospheric model (23) indicates a denser and more expanded atmosphere with an escape rate of  $\sim 3.5 \times 10^{27}$   $N_2$  molecules  $s^{-1}$  and an exobase at  $8 R_P \sim 9600$  km. These are the conditions that were anticipated on arrival at Pluto.

The New Horizons trajectory was designed to provide solar and Earth occultations of Pluto's atmosphere by the ultraviolet spectrometer (Alice) and Radio Science Experiment (REX) instruments, respectively (51, 52). These occultation measurements revealed Pluto's upper atmosphere to be colder and less extended than predicted (2). Matching the Zhu *et al.* (8, 23) model to the New Horizons data suggests a cooler upper atmosphere, composed primarily of methane (rather than nitrogen), with an exobase height of  $2.5 R_P$  and an escape rate of only  $6 \times 10^{25}$  molecules  $s^{-1}$ . This limited atmospheric escape drastically reduces the neutral material upstream of Pluto available for ionization and mass-loading the solar wind.

### Ionosphere

New Horizons did not make a direct measurement of Pluto's ionosphere. Adapting a pre-encounter model of the atmosphere to the density, temperature, and composition measurements from New Horizons (2), we find a peak electron density of  $\leq 1300 \text{ cm}^{-3}$  at a distance of 1900 km =  $1.6 R_P$ . The density drops above this peak with a scale height of  $\sim 330$  km. The main ions are  $H_2CN^+$  (mass = 28 amu) and  $C_2H_5^+$  (mass = 29 amu). Preliminary estimates of the electrical conductivity of such an ionosphere suggest that it is sufficient to sustain currents that would divert the solar wind.

### Bow shock

In modeling interactions (cometary or Mars-like) it is often assumed that the planet's atmosphere and ionosphere and the solar wind can be considered as fluids. For many solar system bodies, fluid descriptions of a plasma-obstacle interaction are often good starting points. Global-scale magnetohydrodynamic (MHD) models have been successful in capturing the basic structure of many plasma interactions. The fast, cold flow of the solar wind in the heliosphere is highly supersonic (Table 1). We illustrate the shape of a Mach 40 shock in Fig. 1 to show how bent such a shock could be behind Pluto. We also show a low Mach number shock to illustrate how including a high density of IPUIs and/or substantial upstream ionization of plutogenic PPUIs would move the

shock farther upstream and reduce the shock angle.

With the IMF being very weak at Pluto's orbital distance, the length scales on which the plasma reacts are large compared with the size of the interaction region. For instance, at 33 AU the gyroradius of solar wind protons is  $\sim 23 R_P$  and the pick-up ion gyroradius of  $CH_4^+$  ions is  $\sim 200$  to  $800 R_P$  (7, 9).

There is no direct evidence of a sharp bow shock in Figs. 2 and 3. This may be because the spacecraft attitude was unfavorable during the passage of the shock (see the gray shading in Fig. 2 and the large angles in Fig. 3) so that it could not be observed well. However, it is important to consider the expected shock thickness. Two thicknesses that have been used in the past are the proton "turn-around" distance and the ion inertial length. For relatively strong magnetic fields, the turn-around distance is approximated by  $V_{sw}/\Omega_{ci}$  (where  $\Omega_{ci}$  is gyrofrequency), which is proportional to  $V_{sw}/B$  (53). High Mach number shocks observed by Voyager at Uranus (54) and Neptune (55), as well as by Cassini at Titan (37), indicate that this is a reasonable approximation, with observed shock widths being  $\sim 30$  to  $70\%$  of this quantity calculated from upstream conditions. For the observed upstream solar wind speed and  $|B|$  of 0.3 nT, we obtain  $\sim 50 R_P$  for a solar wind proton turn-around distance. Perhaps a better scaling for the weak IMF conditions and small obstacle size at Pluto—for which the interaction may be mediated by whistler waves rather than shock-forming MHD modes—is the ion inertial length (53). Again using the measured upstream density of  $\sim 0.025 \text{ cm}^{-3}$ , we get an ion inertial length of  $\sim 1.2 R_P$ . Because the derived 20% slowing interaction distance of  $\sim 6 R_P$  is intermediate between the scaled turn-around and ion inertial lengths, we conclude that an ionospheric obstacle could produce the derived dayside size scale of the solar wind slowing ahead of Pluto.

### Conclusions

Pluto continues to deliver surprises. The New Horizons instruments that measure plasma and particles revealed an interaction region unlike any other body in the solar system and considerably smaller than predicted. This reduced interaction region is possibly due to the combination of a much-smaller-than-expected atmospheric escape rate, as indicated by the New Horizons atmospheric measurements (2), and the flyby occurring during a time of particularly high solar wind flux.

1) Observations indicated enhanced upstream solar wind flux detected by the SWAP instrument. The lack of any slowing until New Horizons was within  $20 R_P$  indicates that almost no heavy ions were ionized within the several thousand  $R_P$  upstream of Pluto. The SWAP data revealed a surprisingly small interaction region, confined on its upwind side to within  $\sim 6 R_P$  of Pluto. The interaction persists to a distance of more than  $400 R_P$  behind Pluto.

2) PEPSSI has not detected evidence of plutogenic pick-up ions or energetic electrons in its



energy range within 500  $R_p$  of Pluto, but the interplanetary energetic particle intensities are considerably perturbed by the interaction. Changes in PEPSSI measurements near Pluto's terminator suggest that <10-keV ions are accelerated and/or deflected away from the direction radially from the Sun. PEPSSI observed decreased suprathermal particles in the wake of the interaction region. The particle intensities near Pluto decreased by a factor of ~10 below the heliospheric value and increased with distance downstream.

3) During the encounter, SDC could detect grains with an effective radius greater than ~1.4  $\mu\text{m}$ . Eliminating spurious events, such as thruster firings (leading to events that are not dust impacts), SDC detected one candidate impact in  $\pm 5$  days around closest approach. In this time period, the effective volume carved out by SDC was 0.83  $\text{km}^3$ , leading to a dust density estimate of 1.2  $\text{km}^{-3}$ , with a 90% confidence level range of  $0.6 < n < 4.6 \text{ km}^{-3}$ .

## REFERENCES AND NOTES

1. S. A. Stern *et al.*, The Pluto system: Initial results from its exploration by New Horizons. *Science* **350**, aad1815 (2015). doi: [10.1126/science.aad1815](https://doi.org/10.1126/science.aad1815); pmid: 26472913
2. G. R. Gladstone *et al.*, New Horizons Science Team, The atmosphere of Pluto as observed by New Horizons. *Science* **351**, aad8866 (2016).
3. D. J. McComas *et al.*, The Solar Wind Around Pluto (SWAP) instrument aboard New Horizons. *Space Sci. Rev.* **140**, 261–313 (2008). doi: [10.1007/s11214-007-9205-3](https://doi.org/10.1007/s11214-007-9205-3)
4. R. L. McNutt Jr. *et al.*, The Pluto Energetic Particle Spectrometer Science Investigation (PEPSSI) on the New Horizons Mission. *Space Sci. Rev.* **140**, 315–385 (2008). doi: [10.1007/s11214-008-9436-y](https://doi.org/10.1007/s11214-008-9436-y)
5. M. Horányi *et al.*, The Student Dust Counter on the New Horizons mission. *Space Sci. Rev.* **140**, 387–402 (2008). doi: [10.1007/s11214-007-9250-y](https://doi.org/10.1007/s11214-007-9250-y)
6. F. Bagenal, R. L. McNutt Jr., Pluto's interaction with the solar wind. *Geophys. Res. Lett.* **16**, 1229–1232 (1989). doi: [10.1029/GL016i01p01229](https://doi.org/10.1029/GL016i01p01229)
7. K. Kecskemeti, T. E. Cravens, Pick-up ions at Pluto. *Geophys. Res. Lett.* **20**, 543–546 (1993). doi: [10.1029/93GL00487](https://doi.org/10.1029/93GL00487)
8. F. Bagenal, T. E. Cravens, J. G. Luhmann, R. L. McNutt, A. F. Cheng, in *Pluto and Charon*, S. A. Stern, D. J. Tholan, Eds. (Univ. of Arizona Press, 1997), pp. 523–555.
9. K. Sauer, A. Lipatov, K. Baumgartel, E. Dubinin, Solar wind-Pluto interaction revised. *Adv. Space Res.* **20**, 295–299 (1997). doi: [10.1016/S0273-1177\(97\)00551-6](https://doi.org/10.1016/S0273-1177(97)00551-6)
10. V. I. Shevchenko, S. K. Ride, M. Baine, Wave activity near Pluto. *Geophys. Res. Lett.* **24**, 101–104 (1997). doi: [10.1029/96GL03696](https://doi.org/10.1029/96GL03696)
11. W.-H. Ip, A. Kopp, L. M. Lara, R. Rodrigo, Pluto's ionospheric models and solar wind interaction. *Adv. Space Res.* **26**, 1559–1563 (2000). doi: [10.1016/S0273-1177\(00\)00098-3](https://doi.org/10.1016/S0273-1177(00)00098-3)
12. P. A. Delamere, F. Bagenal, Pluto's kinetic interaction with the solar wind. *Geophys. Res. Lett.* **31**, L04807 (2004). doi: [10.1029/2003GL018122](https://doi.org/10.1029/2003GL018122)
13. E. M. Harnett, R. M. Winglee, P. A. Delamere, Three-dimensional multi-fluid simulations of Pluto's magnetosphere: A comparison to 3D hybrid simulations. *Geophys. Res. Lett.* **32**, L19104 (2005). doi: [10.1029/2005GL023178](https://doi.org/10.1029/2005GL023178)
14. P. A. Delamere, Hybrid code simulations of the solar wind interaction with Pluto. *J. Geophys. Res.* **114**, A03220 (2009). doi: [10.1029/2008JA013756](https://doi.org/10.1029/2008JA013756)
15. T. E. Cravens, D. F. Strobel, Pluto's solar wind interaction: Collisional effects. *Icarus* **246**, 303–309 (2015). doi: [10.1016/j.icarus.2014.04.011](https://doi.org/10.1016/j.icarus.2014.04.011)
16. D. M. Hunten, A. J. Watson, Stability of Pluto's atmosphere. *Icarus* **51**, 665–667 (1982). doi: [10.1016/0019-1035\(82\)90155-5](https://doi.org/10.1016/0019-1035(82)90155-5)
17. R. L. McNutt Jr., Models of Pluto's upper atmosphere. *Geophys. Res. Lett.* **16**, 1225–1228 (1989). doi: [10.1029/GL016i01p01225](https://doi.org/10.1029/GL016i01p01225)
18. V. A. Krasnopolsky, Hydrodynamic flow of  $\text{N}_2$  from Pluto. *J. Geophys. Res.* **104**, 5955–5962 (1999). doi: [10.1029/1998JE000052](https://doi.org/10.1029/1998JE000052)
19. F. Tian, O. B. Toon, Hydrodynamic escape of nitrogen from Pluto. *Geophys. Res. Lett.* **32**, L18201 (2005). doi: [10.1029/2005GL023510](https://doi.org/10.1029/2005GL023510)
20. D. F. Strobel,  $\text{N}_2$  escape rates from Pluto's atmosphere. *Icarus* **193**, 612–619 (2008). doi: [10.1016/j.icarus.2007.08.021](https://doi.org/10.1016/j.icarus.2007.08.021)
21. O. J. Tucker, J. T. Erwin, J. I. Deighan, A. N. Volkov, R. E. Johnson, Thermally driven escape from Pluto's atmosphere: A combined fluid/kinetic model. *Icarus* **217**, 408–415 (2012). doi: [10.1016/j.icarus.2011.11.017](https://doi.org/10.1016/j.icarus.2011.11.017)
22. O. J. Tucker, R. E. Johnson, L. A. Young, Gas transfer in the Pluto-Charon system: Charon atmosphere. *Icarus* **246**, 291–297 (2015). doi: [10.1016/j.icarus.2014.05.002](https://doi.org/10.1016/j.icarus.2014.05.002)
23. X. Zhu, D. F. Strobel, J. T. Erwin, The density and thermal structure of Pluto's atmosphere and associated escape processes and rates. *Icarus* **228**, 301–314 (2014). doi: [10.1016/j.icarus.2013.10.011](https://doi.org/10.1016/j.icarus.2013.10.011)
24. F. Bagenal *et al.*, Solar wind at 33 AU: Setting bounds on the Pluto interaction for New Horizons. *J. Geophys. Res.* **120**, 1497–1511 (2015). doi: [10.1002/2015JE004880](https://doi.org/10.1002/2015JE004880)
25. D. J. McComas *et al.*, Diverse plasma populations and structures in Jupiter's magnetotail. *Science* **318**, 217–220 (2007). doi: [10.1126/science.1147393](https://doi.org/10.1126/science.1147393); pmid: 17932282
26. R. W. Ebert, D. J. McComas, F. Bagenal, H. A. Elliott, Location, structure, and motion of Jupiter's dusk magnetospheric boundary from ~1625 to 2550  $R_J$ . *J. Geophys. Res.* **115**, A12223 (2010). doi: [10.1029/2010JA015938](https://doi.org/10.1029/2010JA015938)
27. G. Nicolaou, D. J. McComas, F. Bagenal, H. A. Elliott, Properties of plasma ions in the distant Jovian magnetosheath using Solar Wind Around Pluto (SWAP) data on New Horizons. *J. Geophys. Res.* **119**, 3463–3479 (2014).
28. G. Nicolaou, D. J. McComas, F. Bagenal, H. A. Elliott, R. W. Ebert, Jupiter's deep magnetotail boundary layer. *Planet. Space Sci.* **111**, 116–125 (2015). doi: [10.1016/j.pss.2015.03.020](https://doi.org/10.1016/j.pss.2015.03.020)
29. G. Nicolaou, D. J. McComas, F. Bagenal, H. A. Elliott, R. J. Wilson, Plasma properties in the deep Jovian magnetotail. *Planet. Space Sci.* **119**, 222–232 (2015). doi: [10.1016/j.pss.2015.10.001](https://doi.org/10.1016/j.pss.2015.10.001)
30. H. A. Elliott *et al.*, <http://arxiv.org/abs/1601.07156> (2016).
31. B. M. Randol, H. A. Elliott, J. T. Gosling, D. J. McComas, N. A. Schwadron, Observations of isotropic interstellar pick-up ions at 11 and 17 AU from New Horizons. *Astrophys. J.* **755**, 75–82 (2012). doi: [10.1088/0004-637X/755/1/75](https://doi.org/10.1088/0004-637X/755/1/75)
32. B. M. Randol, D. J. McComas, N. A. Schwadron, Interstellar pick-up ions observed between 11 and 22 AU by New Horizons. *Astrophys. J.* **768**, 120–128 (2013). doi: [10.1088/0004-637X/768/2/120](https://doi.org/10.1088/0004-637X/768/2/120)
33. J. D. Richardson, C. Wang, L. F. Burlaga, Correlated solar wind speed, density, and magnetic field changes at Voyager 2. *Geophys. Res. Lett.* **30**, 2207 (2003). doi: [10.1029/2003GL018253](https://doi.org/10.1029/2003GL018253)
34. Note that these values are updated from (4).
35. L. Villanueva, R. L. McNutt Jr., A. J. Lazarus, J. T. Steinberg, Voyager observations of  $\text{O}^{6+}$  and other minor ions in the solar wind. *J. Geophys. Res.* **99**, 2553–2565 (1994). doi: [10.1029/92JA02899](https://doi.org/10.1029/92JA02899)
36. M. E. Hill, N. A. Schwadron, D. C. Hamilton, R. D. DiFabio, R. K. Squier, Interplanetary suprathermal  $\text{He}^+$  and  $\text{He}^{++}$  observations during quiet periods from 1 to 9 AU and implications for particle acceleration. *Astrophys. J.* **699**, L26–L30 (2009). doi: [10.1088/0004-637X/699/1/L26](https://doi.org/10.1088/0004-637X/699/1/L26)
37. C. Bertucci *et al.*, Titan's interaction with the supersonic solar wind. *Geophys. Res. Lett.* **42**, 193–200 (2015). doi: [10.1002/2014GL02106](https://doi.org/10.1002/2014GL02106)
38. D. Clack, J. C. Kasper, A. J. Lazarus, J. T. Steinberg, W. M. Farrell, Wind observations of extreme ion temperature anisotropies in the lunar wake. *Geophys. Res. Lett.* **31**, L06812 (2004). doi: [10.1029/2003GL018298](https://doi.org/10.1029/2003GL018298)
39. A. R. Poppe, D. James, B. Jacobsmeier, M. Horányi, First results from the Venetia Burney Student Dust Counter on the New Horizons mission. *Geophys. Res. Lett.* **37**, L11101 (2010). doi: [10.1029/2010GL043300](https://doi.org/10.1029/2010GL043300)
40. J. R. Szalay, M. Piquette, M. Horányi, The Student Dust Counter: Status report at 23 AU. *Earth Planets Space* **65**, 1145–1149 (2013). doi: [10.5047/eps.2013.02.005](https://doi.org/10.5047/eps.2013.02.005)
41. D. Han, A. R. Poppe, M. Piquette, E. Grun, M. Horányi, Constraints on dust production in the Edgeworth-Kuiper Belt from Pioneer 10 and New Horizons measurements. *Geophys. Res. Lett.* **38**, L24102 (2011). doi: [10.1029/2011GL050136](https://doi.org/10.1029/2011GL050136)
42. A. R. Poppe, An improved model for interplanetary dust fluxes in the outer solar system. *Icarus* **264**, 369–386 (2016). doi: [10.1016/j.icarus.2015.10.001](https://doi.org/10.1016/j.icarus.2015.10.001)
43. D. A. Gurnett, J. A. Anshor, W. S. Kurth, L. J. Granroth, Micron-sized dust particles detected in the outer solar system by the Voyager 1 and 2 plasma wave instruments. *Geophys. Res. Lett.* **24**, 3125–3128 (1997). doi: [10.1029/97GL03228](https://doi.org/10.1029/97GL03228)
44. N. J. T. Edberg *et al.*, Magnetosonic Mach number effect of the position of the bow shock at Mars in comparison to Venus. *J. Geophys. Res.* **115**, A07203 (2010). doi: [10.1029/2009JA014998](https://doi.org/10.1029/2009JA014998)
45. H. Nilsson *et al.*, Birth of a comet magnetosphere: A spring of water ions. *Science* **347**, aaa0571 (2015). doi: [10.1126/science.aaa0571](https://doi.org/10.1126/science.aaa0571); pmid: 25613894
46. H. Nilsson *et al.*, Evolution of the ion environment of comet 67P/Churyumov-Gerasimenko - Observations between 3.6 and 2.0 AU. *Astron. Astrophys.* **583**, A20 (2015). doi: [10.1051/0004-6361/201526142](https://doi.org/10.1051/0004-6361/201526142)
47. T. W. Broiles *et al.*, Rosetta observations of solar wind interaction with the comet 67P/Churyumov-Gerasimenko. *Astron. Astrophys.* **583**, A21 (2015). doi: [10.1051/0004-6361/201526046](https://doi.org/10.1051/0004-6361/201526046)
48. J. L. Elliot *et al.*, Pluto's atmosphere. *Icarus* **77**, 148–170 (1989). doi: [10.1016/0019-1035\(89\)90014-6](https://doi.org/10.1016/0019-1035(89)90014-6)
49. L. A. Young, J. C. Cook, R. V. Yelle, E. F. Young, Upper limits on gaseous CO at Pluto and Triton from high-resolution near-IR spectroscopy. *Icarus* **153**, 148–156 (2001). doi: [10.1006/icar.2001.6662](https://doi.org/10.1006/icar.2001.6662)
50. E. Lellouch *et al.*, Exploring the spatial, temporal, and vertical distribution of methane in Pluto's atmosphere. *Icarus* **246**, 268–278 (2015). doi: [10.1016/j.icarus.2014.03.027](https://doi.org/10.1016/j.icarus.2014.03.027)
51. S. A. Stern, The New Horizons Pluto Kuiper Belt mission: An overview with historical context. *Space Sci. Rev.* **140**, 3–21 (2008). doi: [10.1007/s11214-007-9295-y](https://doi.org/10.1007/s11214-007-9295-y)
52. L. A. Young *et al.*, New Horizons: Anticipated scientific investigations at the Pluto system. *Space Sci. Rev.* **140**, 93–127 (2008). doi: [10.1007/s11214-008-9462-9](https://doi.org/10.1007/s11214-008-9462-9)
53. S. J. Schwartz, M. F. Thomsen, J. T. Gosling, Ions upstream of the Earth's bow shock: A theoretical comparison of alternative source populations. *J. Geophys. Res.* **88**, 2039–2047 (1983). doi: [10.1029/JA088iA03p02039](https://doi.org/10.1029/JA088iA03p02039)
54. F. Bagenal, J. W. Belcher, E. C. Sittler Jr., R. P. Lepping Jr., The Uranian bow shock: Voyager 2 inbound observations of a high Mach number shock. *J. Geophys. Res.* **92**, 8603–8612 (1987). doi: [10.1029/JA092iA08p08603](https://doi.org/10.1029/JA092iA08p08603)
55. A. Szabo, R. P. Lepping, Neptune inbound bow shock. *J. Geophys. Res.* **100**, 1723–1730 (1995). doi: [10.1029/94JA02491](https://doi.org/10.1029/94JA02491)
56. D. J. McComas, H. A. Elliott, N. A. Schwadron, Pickup hydrogen distributions in the solar wind at ~11 AU: Do we understand pickup ions in the outer heliosphere? *J. Geophys. Res.* **115**, A03102 (2010). doi: [10.1029/2009JA014604](https://doi.org/10.1029/2009JA014604)

## ACKNOWLEDGMENTS

We thank the many contributors to the development of the SDC, SWAP, and PEPSSI instruments and acknowledge many useful discussions with colleagues. The New Horizons mission is supported by NASA's New Frontiers Program. S.A.S. is also affiliated with Florida Space Institute, Uwingu, Golden Spike, and World View Enterprises. A.R.P. acknowledges support from NASA's Planetary Atmospheres Program (grant NNX13AG55G). As contractually agreed to with NASA, fully calibrated New Horizons Pluto system data will be released via the NASA Planetary Data System (<https://pds.nasa.gov/>) in a series of stages in 2016 and 2017 as the data set is fully downlinked and calibrated.

## SUPPLEMENTARY MATERIALS

[www.sciencemag.org/content/351/6279/aad9045/suppl/DC1](http://www.sciencemag.org/content/351/6279/aad9045/suppl/DC1)  
Materials and Methods  
Supplementary Text  
Figs. S1 and S2  
References (57–59)  
New Horizons Science Team Author List

18 November 2015; accepted 29 January 2016  
10.1126/science.aad9045